Influence of Peak Pressure and Temperature on the Structure/Property Response of Shock-Loaded Ta and Ta-10W

GEORGE T. GRAY III and KENNETH S. VECCHIO

The deformation behavior and substructure evolution of unalloyed-Ta and Ta-10W under quasistatic conditions have been compared to their respective responses when shock prestrained to 20 GPa at 25 °C as well as to unalloyed-Ta shocked to 7 GPa at 25 °C, 200 °C, and 400 °C. The reload yield behavior of shock-prestrained Ta and Ta-10W did not exhibit enhanced shock hardening when compared to their respective quasistatic stress-strain response at an equivalent strain level. In addition, the reload yield behavior of Ta shock prestrained to 7 GPa at 200 °C or 400 °C was found to exhibit increased hardening compared to the shock prestraining at 25 °C. The quasistatic substructure evolution and shock-hardening responses of Ta and Ta-10W were investigated *via* transmission electron microscopy (TEM). The dislocation substructures in both materials and at each strain rate condition and temperature were similar and consisted primarily of long, straight, $(a/2)\langle 111\rangle$ type screw dislocations. The propensity for long, straight screw dislocations, irrespective of the loading condition, supports the theory of strong Peierls stress control on defect generation and defect storage. The substructure evolution and mechanical behavior of Ta and Ta-10W are discussed in terms of defect storage mechanisms and compared to the mechanisms operative in face-centered cubic (fcc) metals.

I. INTRODUCTION

THE passage of shock waves through materials has been known since the 1940s to alter to varying degrees the structure/property response of a broad range of metals and alloys. Specific examples of postshock response in a wide variety of materials as a function of the applied shock parameters have been reviewed previously by a number of authors.[1–6] These effects have been particularly well documented for a large number of face-centered-cubic (fcc) metals, such as copper, nickel, and aluminum, and fcc alloys including brass and austenitic stainless steels. Shock response studies on body-centered-cubic (bcc) metals have preferentially focused on iron and ferritic steels due to extensive interest in the α-ε pressure-induced phase transition.[2,3] Considerably fewer studies have been undertaken on other pure bcc metals, such as niobium, molybdenum, tantalum, and tungsten.[1,3] Shock-loaded fcc metals and alloys have been repeatedly shown to exhibit increased yield strengths and hardness values in mechanical tests following shock prestraining compared to the same metal deformed at a low strain rate to an equivalent plastic strain level.[1–6] Figure 1 illustrates an example of the substantially increased reload yield strength response for shock-prestrained high-purity copper (Cu) and nickel (Ni-270).[7,8] In this figure, the stress-strain responses of the shock-prestrained Cu and Ni-270, measured quasistatically after recovery, have been offset with respect to the annealed starting material responses at a low strain rate by an amount equal to the transient strain generated by the shock. The shock transient strain is defined here as 4/3 ln (V/V_0), where V and V_0 are the final and initial volumes of Cu and Ni-270 during the shock cycle as determined by their known equation-of-state.[9]

While fcc, bcc, and hexagonal close-packed (hcp) metals exhibit a large number of similarities in their general properties as metals, significant differences in their conventional mechanical responses are recognized. For example, annealed bcc and hcp metals and alloys exhibit pronounced strain-rate and temperature-dependent yield and flow stresses, unlike annealed fcc metals, whose yield strengths show a weak dependence on these variables.[10,11] This dependence in bcc and hcp metals is due to their strong inherent lattice resistance (called the Peierls–Nabarro force or Peierls stress) to dislocation motion compared to fcc metals

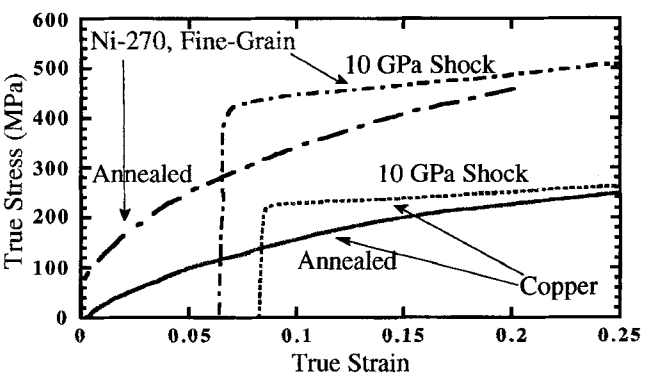

Fig. 1—Reload stress-strain response of shock-loaded Cu and Ni compared to that observed during quasistatic deformation.[7,8]

GEORGE T. GRAY III is Technical Staff Member and Team Leader—Dynamic Properties, Materials Research & Processing Science, with the Los Alamos National Laboratory, Los Alamos, NM 87545. KENNETH S. VECCHIO, Associate Professor, is with the Materials Science Group, Department of Applied Mechanics and Engineering Sciences, University of California–San Diego, La Jolla, CA 92093-0411.

This article is based on a presentation made in the symposium "Dynamic Behavior of Materials," presented at the 1994 Fall Meeting of TMS/ASM in Rosemont, Illinois, October 3–5, 1994, under the auspices of the TMS-SMD Mechanical Metallurgy Committee and the ASM-MSD Flow and Fracture Committee.

Table I. Chemical Composition of Ta and Ta-10W Materials Studied (in Parts per Million)

Alloy	C	O	N	H	Fe	Ni	Cr	W	Nb	Si	Ta
Ta	6	56	24	<1	19	25	9	41	26	—	bal
Ta-10W	15	45	<10	5	<5	<5	<5	9.8*	470	10	bal

*This value is in weight percent not parts per million.

in which the lattice resistance is small.[10] This feature of bcc and hcp metals leads to the observation that stress increments corresponding to a fixed change in strain rate or temperature do not vary systematically with strain contrary to fcc metals. Overcoming these lattice-based obstacles through thermally activated processes therefore becomes a critical factor in understanding the mechanical behavior and substructure evolution of bcc and hcp metals. This is particularly important under very high-rate or shock-loading environments, where thermally activated processes are suppressed.

Recently, the deformation behavior of bcc refractory metals, in particular, tantalum, has received increased interest for ballistic applications.[12–21] While the detailed response of refractory metals to a wide range of deformation paths has been widely examined, systematic studies of the shock response of the refractory metals has received limited attention. Early work by Dieter[1] in 1961 showed that bcc metals other than iron exhibited no or minimal improvement in overall mechanical properties following shock prestraining. Only iron, which displays an allotropic pressure-induced phase transition coupled with extensive deformation twinning during shock deformation shows a pronounced effect of shock loading on defect storage and hence postshock yield and hardness values. High-purity niobium, which exhibits no pressure-induced phase transitions and revealed minimal twinning upon shock prestraining, displayed virtually no increased hardening compared to quasistatic rolling to equivalent strain levels.[1] Recent emphasis has been focused on understanding and modeling the influence of shock loading on defect generation of tantalum and tantalum alloys.[22–31] The purpose of this article is to report results of a systematic study of the influence of peak pressure and temperature on the substructure evolution and mechanical behavior of quasistatically deformed and shock-loaded unalloyed-Ta and Ta-10W.

II. EXPERIMENTAL MATERIALS AND TECHNIQUES

Commercially pure (triple-electron-beam) annealed unalloyed-Ta plate 5-mm thick, supplied by Fansteel Corporation, and Ta-10W plate 10.2-mm thick, supplied by Cabot Corporation, Boyertown, PA, were used in this study;[12] their analyzed chemical compositions are listed in Table I. Both materials were studied in an annealed condition and possessed equiaxed grain structures of ~68- and 73-μm grain sizes for the unalloyed-Ta and Ta-10W, respectively.

Shock recovery experiments were performed using an 80-mm single-stage launcher and recovery techniques as described in detail previously.[3,32] The specimen assembly consisted of a 5.08-mm-thick, 38-mm-diameter sample, stacked behind a 38-mm-diameter, 2.54-mm-thick cover plate which was slip fit, *i.e.*, 0.0254-mm clearance, into a similarly sized bored recess on top of a 7 deg tapered, 12.7-mm-thick, inner momentum disk. The sample was protected from spallation by backing the central momentum disc with a 3.8-mm-thick spall plate. The central disk and spall plate were further surrounded by two concentric momentum trapping rings with outside diameters of 69.8 and 82.5 mm. The two outer momentum trapping rings were interference fit together, and molybdenum disulfide grease was used during assembly of the trapping rings to remove air gaps in the assembly and to facilitate ring separation during recovery.

After assembly, the front surface of the specimen fixture was "skim cut" in a lath to assure the cover plate and momentum rings were flat and perpendicular to the assembly outer circumference to better than 0.0254-mm tolerance. To increase the strength of the shock assembly surrounding the sample, the central momentum disc, outer momentum trapping rings, and spall plate were all fabricated from Ta-2 wt pct W material. While not significantly affecting radial release effects through the use of an alloy of similar shock impedance, this technique significantly reduces bending during deceleration after shock loading, ensuring low residual strains in the shock-recovered materials.[3] Experimental results for recovered samples from various assembly designs have illustrated that assembly tolerances are of primary importance in reducing lateral wave effects. The use of lubricants was also beneficial, although the effect was less prominent.[32] The addition of a cover plate was observed to consistently improve the overall surface finish of the recovered sample.

Tantalum samples were shock loaded to a peak pressure of 7 or 20 GPa for 1-μs pulse duration by impacting the specimen assemblies with 1.9-mm-thick flyer plates at velocities of 235 and 630 m/s, respectively. Soft recovery and simultaneous cooling were achieved by decelerating the central momentum disc containing the sample in a water-catch chamber positioned immediately behind the impact area.[3] Following shock loading, the recovered samples were flat and possessed residual plastic strains of ~1.0 to 1.2 pct for the 7 GPa shocks and ~1.8 pct for the 20 GPa shock. The residual shock strain is defined here as the starting sample thickness minus the recovered sample thickness following shock loading divided by the starting sample thickness. These low levels of residual strain are consistent with previous studies which systematically documented the importance of minimizing late-time lateral release driven plastic work on postshock structure-property behavior.[32]

Elevated temperature shock-loading experiments at 7 GPa were conducted at nominally 220 °C and 400 °C using a molybdenum coil resistive heating-element furnace placed circumferentially around the outer momentum trapping ring of the assembly. The temperature of the shock assembly

Fig. 2—Optical micrographs of (*a*) annealed unalloyed-Ta, (*b*) annealed Ta-10W, (*c*) unalloyed-Ta shock loaded to 20 GPa, and (*d*) Ta-10W shock loaded to 20 GPa. Note the presence of deformation twins (arrows) introduced by the shock deformation. The wavy background structure observed in the Ta-10W samples is due to tungsten compositional fluctuations in the annealed plate material which result in differential etching behavior.

was monitored during preheating *via* a thermocouple spot welded to the center of the rear surface of the spall plate. The shock assembly was heated to the desired temperature and held for approximately 5 minutes to ensure uniform temperature. The measured temperatures of the shock fixture just prior to impact were 218 °C and 410 °C, respectively.

Cylindrical compression samples, 6.35-mm diameter by 6.35-mm long, were electrode-discharge machined from the as-received (annealed) and shocked unalloyed-Ta and Ta-10W samples. The mechanical response at 25 °C was measured at a quasistatic strain rate of 0.001 s^{-1}, using a screw-driven Instron testing machine, and dynamically, at a nominal strain rate of 3000 s^{-1}, using a Split–Hopkinson pressure bar.[28] The inherent oscillations in the dynamic stress-strain curves generated by this approach are due to elastic wave dispersion effects in the Hopkinson bars. Unless strain gages are fixed on the samples directly, the elastic wave dispersion effects, as well as the lack of stress equilibrium at low strains (<2 pct plastic strain), make yield strength determinations from Hopkinson bar data inaccurate.[28] As such, only postyield data are presented here.

Metallographic sections of both the annealed and shock-loaded materials were prepared using standard metallographic techniques. The grain structure was revealed by etching in a solution of 2 parts water, 2 parts HNO_3, 2 parts HCl, and 1 part HF; micrographs were obtained using polarized light. The substructures of the unalloyed-Ta and Ta-10W following compression testing or shock prestraining were examined using transmission electron microscopy (TEM). Samples were sectioned parallel to the loading direction using a low-speed diamond saw and the slices were mechanically thinned. The TEM foils were electrochemically polished in a Struers Tenapol III jet-electropolisher to electron transparency using a solution of 600 mL methanol, 30 mL H_2SO_4, and 15 mL HF at −35 °C with an applied voltage of 80 V and 300 mA current. Characterization was performed using a PHILIPS* CM-30 TEM equipped with a double-tilt stage at an accelerating voltage of 300 kV. Dislocation analysis was conducted under a number of two-beam diffraction conditions, and micrographs for g = [200] are presented here.

*PHILIPS is a trademark of Philips Electronic Instruments Corp., Mahwah, NJ.

Compositional analysis of the Ta-10W material was conducted using wavelength dispersive X-ray spectroscopy in a JEOL* 733 microprobe. Pure elemental standards of Ta and W were used for quantification. A beam current of 50 nA and operating potential of 15 kV were used in conjunction with two LiF crystal spectrometers. A beam position step size of 1 μm was used to perform a line trace both normal to the plate surface and parallel to the observed striations. Correlation of the analysis locations to the microstructure was conducted by using microhardness indentations as position markers.

*JEOL is a trademark of Japan Electron Optics Ltd., Tokyo.

III. EXPERIMENTAL RESULTS

A. *Mechanical Response*

Figure 2 shows optical micrographs of unalloyed-Ta and Ta-10W in the annealed condition and shock loaded to 20 GPa at room temperature. The annealed materials have fairly equiaxed grains with uniform contrast in the unalloyed-Ta, but a periodic, wavy background structure is observed in the Ta-10W material. The alternating contrast observed optically (Figure 2(b)) in the Ta-10W was determined to be the result of small tungsten compositional variations parallel to the plate surface. Microprobe measurements across a flat-polished Ta-10W section found that compositional variations, on the order of ±0.5 wt pct W from the nominal composition, correlated with the wavylike striations seen in Figure 2(b). Microprobe measurements made within a striation along a trace parallel to the striation (*i.e.*, parallel to the plate surface) showed only a ±0.05 wt pct W variation, which is approximately the measured accuracy of the analysis. This minor compositional variation from one striation to another, while producing no discernible effect on mechanical behavior, is sufficient to affect etching conditions, thereby altering the local surface relief resulting in the periodic optical contrast. A limited amount of deformation twinning can also be observed in each material as a result of the shock loading. No other significant microstructural changes could be discerned at this level of examination.

The reload mechanical response of shock-prestrained tantalum was found to depend on both the peak shock pressure

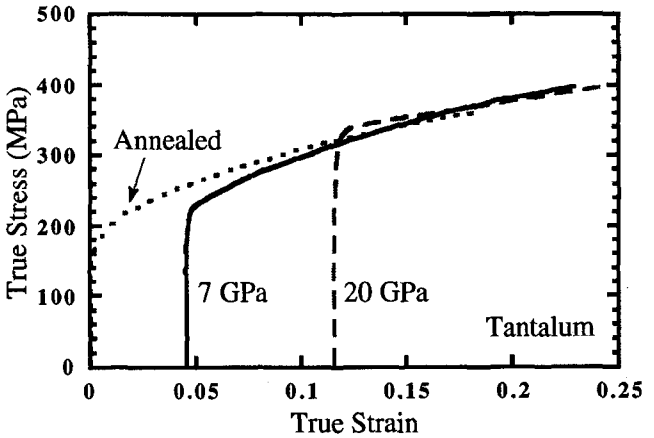

Fig. 3—Quasistatic stress-strain response of shock-recovered Ta after 7 and 20 GPa shocks. Reload curves are offset on the strain axis by the transient strains due to the shock prestrain.

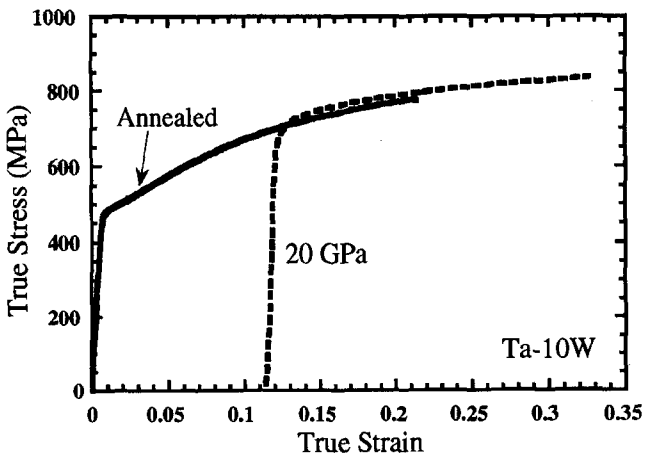

Fig. 4—Quasistatic stress-strain response of shock-recovered Ta-10W after 20 GPa shock. The reload curve is offset on the strain axis by the transient strain due to the shock prestrain.

and the temperature at which shock prestraining was performed. Figure 3 presents a plot of the quasistatic stress-strain behavior of the annealed unalloyed-Ta, as well as the reload behavior of unalloyed-Ta samples shock loaded at room temperature to 7 and 20 GPa. A similar plot of the stress-strain response of shock prestrained Ta-10W and the annealed Ta-10W constitutive behavior is shown in Figure 4. Figure 5 shows a plot of the unalloyed-Ta shock-prestrained samples reloaded dynamically at a strain rate of 3000 s^{-1}. The reload stress-strain curves in Figures 3 through 5 have been offset on the strain axis by the transient strain generated by the shocks. Contrary to the results reviewed for Cu and Ni in Figure 1, unalloyed-Ta shocked to 7 and 20 GPa and Ta-10W shocked to 20 GPa do not exhibit an increased shock-hardening response compared to each material when compared to their quasistatic deformation to an equivalent strain level. This finding is similar to that previously reported for tantalum shock loaded at 25 °C to 15 GPa.[22]

The reload mechanical response of the unalloyed-Ta following shock prestraining to 7 GPa exhibits a slightly reduced flow stress level compared to the quasistatic loading path. The 20 GPa reload stress-strain curves for both the unalloyed-Ta and Ta-10W achieve virtually identical flow stresses (or slightly higher for the unalloyed-Ta) and similar

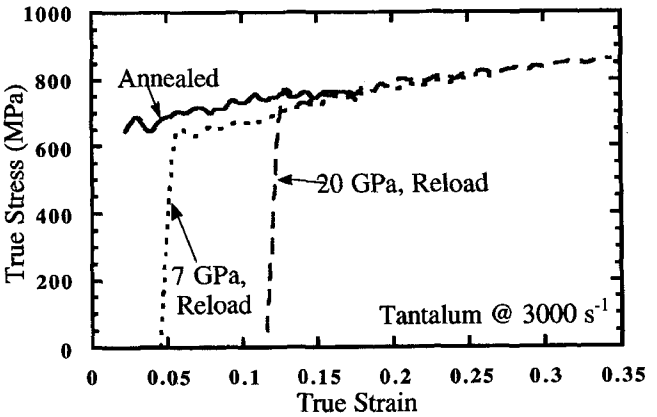

Fig. 5—High-strain-rate reload stress-strain response of shock-prestrained unalloyed-Ta.

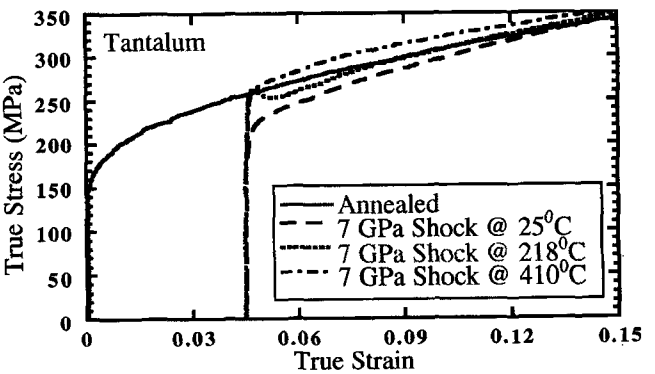

Fig. 6—Reload stress-strain response of unalloyed-Ta shock prestrained to 7 GPa at three different temperatures.

hardening paths as the low-rate-annealed responses of each material at equivalent strain levels. The dynamic reload stress-strain response in Figure 5 shows the same response as that seen in the quasistatic reloads (Figure 4), although the overall flow stress levels are higher in the former case, consistent with the high rate sensitivity of Ta.[13,15] The lack of an enhanced shock-hardening response in unalloyed-Ta and Ta-10W suggested that the mechanism of defect generation and storage is insensitive to the applied strain rate. In addition, these defect generation and storage mechanisms must be significantly different in Ta than those exhibited by Cu or Ni-270.

Given the known strong temperature dependency of defect generation and storage processes in Ta and Ta-alloys,[15] unalloyed-Ta shock assemblies were preheated to elevated temperatures and shock loaded to a peak pressure of 7 GPa. The room-temperature reload stress-strain response of the shock-recovered Ta as a function of shock preheat temperature is shown in Figure 6. Increasing the temperature of shock prestraining (1) increases the postshock reload yield strength of the unalloyed-Ta, (2) affects the postyield hardening response in the 218 °C sample (this sample exhibited a pronounced load drop following yield), and (3) results in work-hardening behavior in the shock-prestrained samples similar to annealed unalloyed-Ta.

B. *Substructure Evolution*

Figure 7 shows TEM micrographs of dislocation substructures in unalloyed-Ta deformed under conditions of

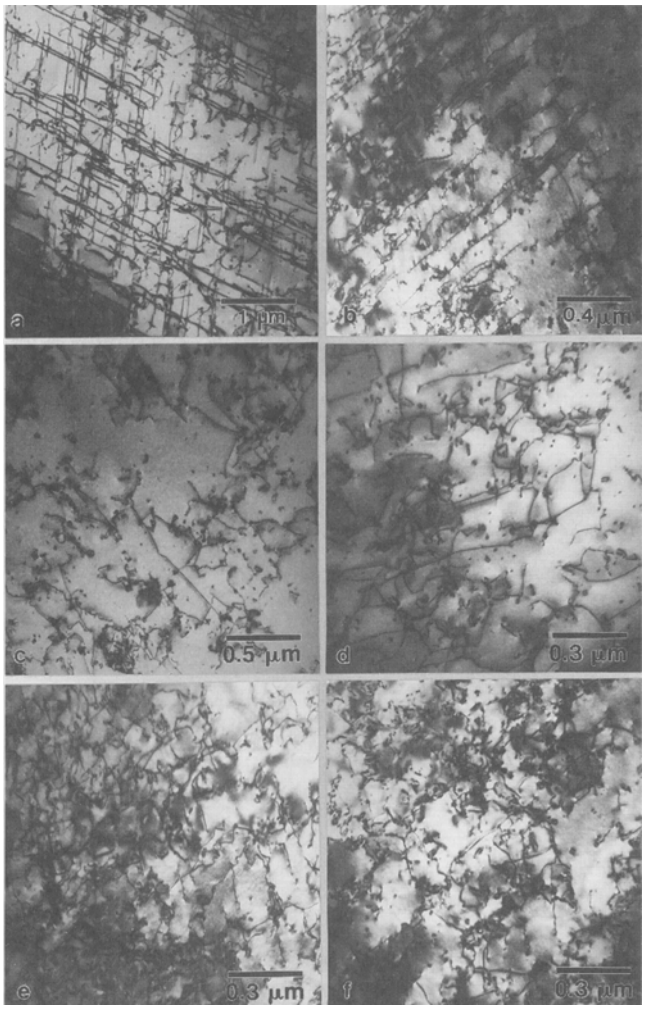

Fig. 7—TEM micrographs showing dislocation substructures of unalloyed-Ta deformed under several strain rates and shock-prestraining conditions: (*a*) deformed in uniaxial compression at a strain rate of 0.001/s to a true plastic strain of ~5 pct; (*b*) deformed in uniaxial compression at a strain rate of 3000/s to a true plastic strain of ~5 pct; (*c*) shock loaded to 7 GPa at room temperature; (*d*) shock loaded to 7 GPa at 218 °C; (*e*) shock loaded to 7 GPa at 410 °C; and (*f*) shock loaded to 20 GPa at room temperature.

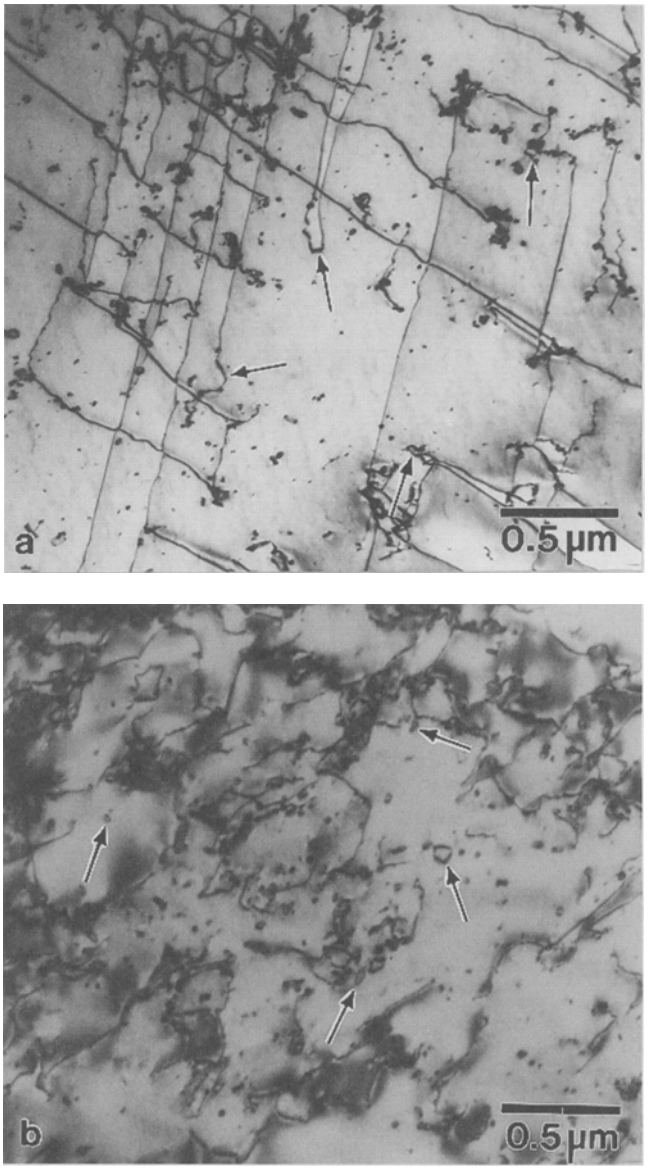

Fig. 8—TEM micrographs of pure Ta shock loaded to 7 GPa shock pressure: (*a*) showing formation of dislocation cusps (arrows) and (*b*) showing dislocation loops and dislocation debris (arrows).

uniaxial compression, either quasistatically or dynamically, and under conditions of shock prestraining to 7 or 20 GPa at various temperatures. The uniaxial compression specimens were deformed to approximately 5 pct strain, which is close to the transient shock strain resulting from a 7 GPa shock in Ta. Contrast analysis of these dislocations was conducted using different *g* reflections under two-beam dynamical conditions. Bright-field images of these dislocations as a function of loading condition obtained using the diffraction vector $\mathbf{g} = [200]$ are presented in Figure 7. The substructures in each micrograph are seen to be very similar and to consist of four types of dislocation features: (a) two sets of long straight screw dislocations, (b) small dislocation cusps on the long straight screw segments (Figure 8(a)), (c) dislocation tangles of mixed character, and (d) small dislocation loops and dislocation debris (Figure 8(b)). The long straight dislocations were determined by $(\mathbf{g} \cdot \mathbf{b})$ analysis to have burgers vectors of $(a/2)\ [1\bar{1}1]$ and $(a/2)\ [\bar{1}\bar{1}1]$, and trace analysis confirmed that the slip plane is (011). There was no residual contrast for $\mathbf{g} \cdot \mathbf{b} = 0$, as well as $\mathbf{g} \cdot \mathbf{b} \wedge u = 0$ (u = line direction of dislocation), and this is an indication that the dislocations are near screw in character. The most notable difference between the dislocation substructure of the uniaxially compressed samples and those of the shock-prestrained samples is the presence of a larger number of dislocation tangles in the shock-loaded samples. Under the high stresses and strain rate of the shocks, a larger number of dislocation nucleation sites are activated, resulting in a more homogeneous distribution of dislocations with a higher probability for tangles. In uniaxial compression, fewer nucleation sites are activated, and more planar arrays of dislocations are produced.

Using tilting experiments in TEM, small cusps of edge character were observed on otherwise long, straight screw dislocations. When the main screw segment was out of contrast (*i.e.*, $\mathbf{g} \cdot \mathbf{b} = 0$), the small cusps of edge character remained in residual contrast ($\mathbf{g} \cdot \mathbf{b} \wedge u \neq 0$). For cubic

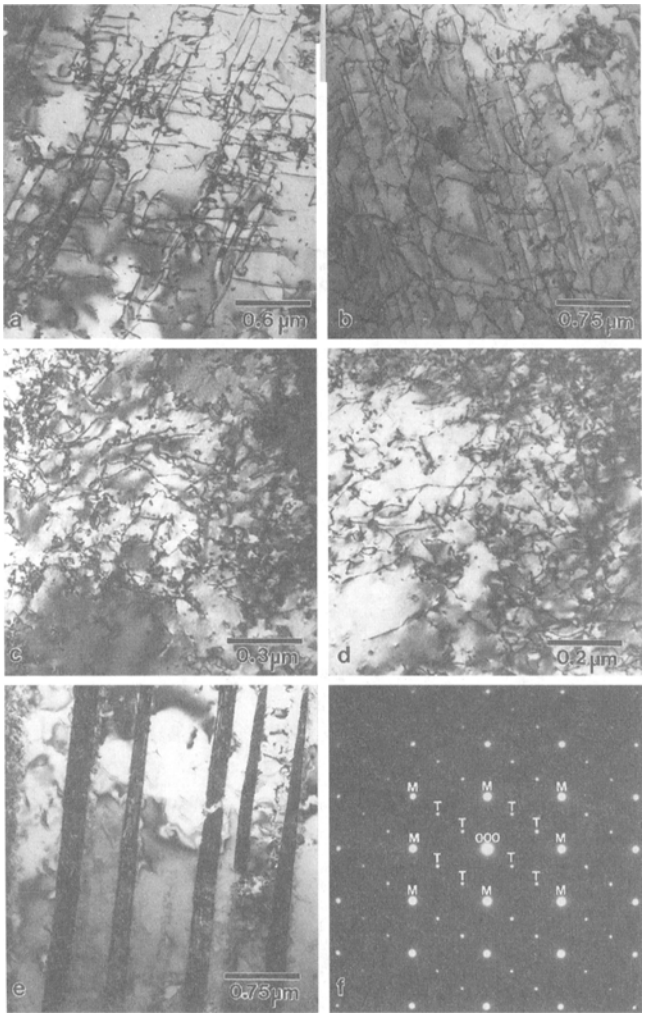

Fig. 9—TEM micrographs of Ta-10W deformed under several strain rates and shock-prestraining conditions: (*a*) deformed in uniaxial compression at a strain rate of 0.001/s to a true plastic strain of ~12 pct; (*b*) deformed in uniaxial compression at a strain rate of 3000/s to a true plastic strain of ~12 pct; (*c*) and (*d*) shock loaded to 20 GPa at room temperature showing dislocation structures; (*e*) shock loaded to 20 GPa at room temperature showing deformation twins; and (*f*) [011] diffraction pattern showing reflections for the deformation twins (T) shown in (e). The twins lie on {112} planes in ⟨111⟩ directions.

crystals, the elastic anisotropy is described by an anisotropy factor (A) given by

$$A = \frac{2C_{44}}{C_{11} - C_{12}}$$

where C_{11}, C_{12}, and C_{44} are elastic stiffness constants. Using the data for the elastic constants for Ta from Bolef[33] of C_{11} = 260.9 GPa, C_{12} = 15.74 GPa, and C_{44} = 8.18 GPa, the anisotropy factor for unalloyed-Ta is 1.58. The anisotropy factor for a perfectly isotropic cubic material is 1 (tungsten = 0.98), and a highly anisotropic cubic material such as Pb has an anisotropy factor of 4.12. As such, tantalum is fairly isotropic and the elastic strain energy of the dislocation does not vary significantly with line direction; the wavy nature of the long dislocations is an indication of the instability of the screw orientations. In addition to the long screw dislocations and their associated debris and loops, some dislocation tangles were also observed which increased in density and number with increasing uniaxial strain or increasing shock pressure. Specimens shock loaded to 20 GPa also exhibited numerous deformation twins, as shown in the optical micrographs of Figure 2.

Figure 9 shows TEM micrographs from the Ta-10W specimens deformed either quasistatically or dynamically under uniaxial compression or subjected to shock prestraining to 20 GPa at room temperature. The uniaxial compression specimens were deformed to a strain of approximately 12 pct, which is close to the transient shock strain achieved when they are shocked to 20 GPa. The substructures in each case are very similar to each other, as well as similar to the unalloyed-Ta substructures. Diffraction analysis of these dislocation structures revealed identical dislocation characters and similar dislocation morphologies with increasing strain. Deformation twins were observed in the shock-loaded specimens, a feature not observed in the uniaxially compressed samples deformed to an equivalent strain. The twins were identified as lying on {112} planes in ⟨111⟩ directions consistent with deformation twins previously observed in tantalum alloys.[34,35]

Low and Turkalo[42] have reported similar dislocation structures in Fe-3 pct Si single crystals, with bcc structure, deformed in compression. Pure screw and mixed segments of dislocations exhibited numerous cusps, whereas the edge dislocations exhibited cusps only very rarely. The cusps in the screw dislocations were frequently associated with resolvable trails of edge dislocations. As a common feature of the dislocation pattern in the slip band, Low and Turkalo observed a large amount of debris, consisting of small, elongated, or equiaxed loops created by plastic deformation. Johnston and Gilman[43] proposed that a moving screw dislocation becomes jogged by cross-slip. The jog segment is not mobile under the applied stress, causing the screw to move. With continuing motion of the original screw dislocation, a trail forms behind the moving dislocation. These trails consist of rows of vacancies or interstitials, or of two edge segments of opposite sign, in planes separated by a distance equal to the height of the jog. With continued motion of the main screw segment, the formation of dipole loops results (Figure 8). The +ve and −ve edge dislocations of the dipole are attracted to each other, and this results in loops pinching off from the main screw segment. The jogs and the cusps in the screw dislocations formed by the drag on the jogged screw dislocations may account for the much lower mobility of screw dislocations as compared to edge dislocations in Fe-3 pct Si reported by Low and Guard,[44] Nb single crystals reported by Bowen *et al.*,[45] and Ta single crystals reported by Spitzig and Mitchell.[46] This type of mechanism is responsible for much of the small dislocation loops and dislocation debris observed in the micrographs of Figures 7 through 9.

IV. DISCUSSION

The postshock mechanical response of unalloyed-Ta and Ta-10W, similar to that described by Dieter for Nb,[1] reveals that increased hardening due to shock prestraining is not observed. The reload flow stress response of shocked unalloyed-Ta does not display the often documented increased defect storage response of shock loading in fcc metals compared to conventional strain-rate loading paths.[3]

This apparent difference between bcc- and fcc-structured metals can be understood through an examination of the different defect storage processes in these two crystal structures.

The increased hardening during shock loading in fcc metals has been qualitatively linked to the subsonic restriction on dislocation velocity, requiring the generation and storage of a larger number of dislocations for a given strain.[3] A strong dependence of the stage II work-hardening rate[8,29] on strain rate in fcc metals (*e.g.*, Cu and Ni-270, Figure 1) supports this fact. This increased hardening response clearly shows that the inherent dislocation-dislocation micromechanisms responsible for defect storage in fcc metals deformed at conventional strain rates are altered under high-strain-rate and shock-wave loading. The exact phenomenon responsible for increased hardening efficiency during shock-wave deformation has yet to be adequately quantitatively explained or modeled.[8,29] However, its manifestation in high stacking fault energy fcc metals suggests that it is linked to both (a) increased dislocation interactions resulting from enhanced dislocation nucleation at the higher stress levels achieved at high strain rates and (b) suppression of dynamic recovery processes, which depend on cross-slip. Cross-slip is made more difficult when deformation occurs at higher strain rates due to reduced thermal activation,[29] and thus, more planar slip results. The absence of shock-enhanced hardening in low-SFE Si-bronze[3] and low-SFE Ni-based 230-alloy[31] is consistent with differences in cross-slip reducing the amount of total defect storage in the shock cycle. More ''homogeneous'' dislocation nucleation or widespread multiplication from existing sources with increasing stress levels at high/shock strain rates is hypothesized to lead to reduced dislocation slip distances prior to tangling with other defects in fcc metals.[3,29] Smaller dislocation cells, and higher hardness and reload yield strength in copper following shock loading, each reflecting an increased dislocation density compared to copper quasistatically to an equivalent strain, support this hypothesis.[2,7,36]

In the case of unalloyed-tantalum, the stage II work-hardening rate is seen to be virtually constant for strain rates of 10^{-4} to 8000 s^{-1} over the temperature range of 77 to 673 K.[12,37] This is in contrast to Ni-270[8] or other pure fcc metals like Cu or Al where the stage II work-hardening rate increases with increasing strain rate or decreasing temperature due to the suppression of dynamic recovery processes.[38] Extrapolation of the quasistatic yield surface to the yield surface exhibited by the postshock reload behavior, *i.e.*, enhanced shock hardening for pure fcc metals, supports a strong rate dependency of structure evolution in these fcc metals. However, no strength enhancement was observed here for Ta or Ta-10W as a result of shock loading, indicating no rate dependency of structure evolution for these bcc alloys. Unlike the shock response of iron, where substantial deformation twinning has been shown to contribute significantly to its shock-hardening response, only minimal twinning occurred in the Ta or Ta-10W at 7 or 20 GPa. The lack of enhanced defect storage in both Nb and the current results on unalloyed-Ta and Ta-10W during shock loading is therefore consistent with this lack of a dependence of the stage II hardening rate in polycrystalline Ta, as discussed previously for fcc metals, and supports defect storage being dislocation drag controlled. Accordingly, defect generation and storage phenomena may be viewed using the framework of dislocation kinetics as is the case for low-rate plasticity.[8,24] The absence of enhanced shock hardening is believed to reflect the influence of the large lattice friction (Peierls stress) component of the flow stress in Ta, Ta-10W, and Nb.[22,24] At low temperatures and high rates, the Peierls stress is a significant portion of the flow stress in bcc metals and alloys (~0.48 GPa shear stress for Ta[39]).

Under high-rate loading, dislocation motion in Ta will be significantly restricted and cross-slip inhibited as a result of the higher Peierls barrier on screw segments, due to their nonplanar dislocation cores,[10,40] than edge segments in bcc metals. Without significant assistance from thermal activation, many of the screw dislocations are limited to conservative motion, and therefore, new dislocation line length is difficult to generate. Although some additional dislocation line length is generated by the formation of edge kinks and jogs in the long screw dislocations, the relative amount of additional line length created is small compared to the line length that can be created by easy cross-slip of screw dislocations in a high stacking fault fcc material. Any restriction on the generation of additional dislocations, per unit of imposed plastic strain, as in the case of enhanced hardening in fcc metals, should decrease the shock-hardening response of Ta and Nb through its effect on the overall rate of defect accumulation.[41]

Analysis of shock-wave profiles in tantalum[25,26,39] supports the importance of dislocation kinetics in describing the thermally activated generation and storage of dislocations in bcc *vs* fcc metals. The general nature of these wave profiles[25,26,39] indicates that substructure evolution is dislocation-drag-controlled above a strong Peierls barrier. When the shock data are examined in terms of the deviatoric stress *vs* plastic strain, little or no difference is observed between the initial and final deviatoric stresses of the shock in Ta.[26] This result suggests a lack of significant work hardening in either unalloyed-Ta or Ta-10W resulting from the shock process. Accordingly, the evolution of the *mobile* dislocation density, evident in the tantalum shock wave results, must involve mostly the freeing and motion of dislocations already present in the microstructure and the addition of relatively few dislocations geometrically necessary to meet the applied strain rate. In contrast, examination of the deviatoric stress *vs* plastic strain for copper subjected to shock loading indicates that a significant and rapid increase in the total dislocation density occurs.[39]

The results presented here showing that above-ambient temperature shock prestraining (218 °C and 410 °C shocks) leads to a higher reload yield strength following the shock suggest that the temperature increase may increase the reload response either by (1) directly increasing defect storage during the shock by increasing thermally activated cross-slip or (2) postshock pinning of the dislocations generated in the shock by mobile interstitials. This pinning effect is aided by thermally activated diffusion of the interstitials, *i.e.*, assisting static strain aging. In the 410 °C shock experiment, the higher postyield stresses sustained in this sample suggest a slightly increased level of defect storage, although definitive evidence to support this assertion is not evident in the substructure. No evidence of a greater

density of dislocation loops or other dislocation debris existed in the shock-recovered samples tested at elevated temperature compared to those tested at room temperature. However, the higher flow stresses exhibited by the sample recovered from the 410 °C shock experiment may also be due to enhanced strain aging associated with the higher diffusivity of the interstitial species at this higher temperature. Since the total interstitial content (O, N, and C) of each alloy is only slightly less than 100 ppm, interstitial pinning effects cannot be overlooked.

The observation of some long straight screw segments in Ta and Ta-alloys following low-temperature deformation or shock deformation is consistent with the Peierls stress affecting defect generation and storage processes in tantalum.[22,24] This reduced cross-slip ability in bcc metals, where defect generation is dominated by dislocation processes, will significantly alter defect storage at high rates or low temperatures, leading to similar hardening behavior from quasistatic to shock-loading rates. The suppression of cross-slip in Ta at shock-loading strain rates will additionally change dislocation motion from "areal" glide, as in fcc metals, to a mixture of areal and "lineal" glide.[38,47] This will tend to decrease the total work hardening over that geometrically necessary to accommodate the applied plastic strain rate by suppressing the storage of significant amounts of new dislocation line length.[47] The combined contributions of the Peierls dominance and its effect on new dislocation storage suggest that a large percentage of the applied strain rate of the shock in nontwinning bcc metals must be accommodated by a very active mobile dislocation population. This is in contrast to the ever increasing stored dislocation density in fcc metals related to widespread dislocation nucleation and multiplication, but which are easily locked, as supported by enhanced shock hardening in fcc metals.[3,29] These observations are consistent with the differences in the rate sensitivity of defect storage between fcc and bcc materials under nonshock deformation conditions.

V. SUMMARY AND CONCLUSIONS

Based upon a study of the variation of peak shock pressure and the temperature at which shock prestraining was conducted on the mechanical response of unalloyed-Ta and Ta-10W, the following conclusions can be drawn.

1. the reload yield behavior of shock-prestrained unalloyed-Ta and Ta-10W does not exhibit enhanced shock hardening compared to quasistatic or dynamic deformation to an equivalent strain level; the absence of shock-enhanced hardening in Ta is consistent with the lack of a dependence of the stage II hardening rate in polycrystalline Ta and Ta-10W on strain rate.
2. The postshock mechanical response and substructure in tantalum are consistent with defect generation and storage mechanisms being dislocation-drag-controlled above a strong Peierls barrier with evolution of the mobile dislocation density, while the total dislocation density increases only slowly; this interpretation is also consistent with wave-profile analysis of the shock front in tantalum.[25,26,39]
3. The reload yield behavior of unalloyed-Ta shock prestrained to 7 GPa at 218 °C or 410 °C exhibits increased hardening compared to shock prestraining at 25 °C; these increases are consistent with strain aging and increased dislocation storage due to thermally activated processes for the 218 °C and 400 °C prestrains, respectively.

ACKNOWLEDGMENTS

The authors wish to acknowledge C. Trujillo, W. Wright, and M.F. Lopez for their assistance with the experimental aspects of this study. The work at Los Alamos National Laboratory was performed under the auspices of the United States Department of Energy. The work performed at UCSD was supported through a University Research Initiative (URI) awarded by the Army Research Office under Contract No. ARO-DAAL-03-92-G-0108.

REFERENCES

1. G.E. Dieter: *Response of Metals to High Velocity Deformation*, Interscience Publishers, New York, NY, 1961, pp. 409-45.
2. L.E. Murr: in *Shock Waves and High Strain Rate Phenomena in Metals*, M.A. Meyers and L.E. Murr, eds., Plenum Press, New York, NY, 1981, pp. 607-73.
3. G.T. Gray: in *High Pressure Shock Compression of Solids*, J.R. Asay and M. Shahinpoor, eds., Springer-Verlag, New York, NY, 1993, pp. 187-215.
4. W.C. Leslie: *Metallurgical Effects at High Strain Rates*, Plenum Press, New York, NY, 1973, p. 571.
5. S. Mahajan: *Phys. Status Solidi A*, 1970, vol. 2, pp. 187-201.
6. M.A. Mogilevsky and P.E. Newman: *Phys. Rep.*, 1983, vol. 97, pp. 357-93.
7. G.T. Gray and P.S. Follansbee: in *Impact Loading and Dynamic Behavior of Materials*, C.Y. Chiem, H.-D. Kunze, and L.W. Meyer, eds., Deutsche Gesellschaft fuer Metallkunde, Oberursel, Germany, 1988, vol. 2, pp. 541-48.
8. P.S. Follansbee and G.T. Gray: *Int. J. Plasticity*, 1991, vol. 7, pp. 651-60.
9. R.G. McQueen and S.P. Marsh: *J. Appl. Phys.*, 1960, vol. 31, pp. 1253-69.
10. V. Vitek: *Dislocations and Properties of Real Materials*, Institute of Metals, London, 1985, vol. 323, pp. 30-50.
11. J.W. Christian: *Metall. Trans. A*, 1983, vol. 14A, pp. 1237-56.
12. G.T. Gray, S. Bingert, S.I. Wright, and S.R. Chen: in *High-Temperature Silicides and Refractory Alloys*, C.L. Briant, J.J. Petrovic, B.P. Bewlay, A.K. Vasudevan, and H.A. Lipsitt, eds., Materials Research Society, Pittsburgh, PA, 1994, vol. 322, pp. 407-12.
13. G.T. Gray and A.D. Rollett: in *High Strain Rate Behavior of Refractory Metals and Alloys*, R. Asfahani, E. Chen, and A. Crowson, eds., TMS-AIME, Warrendale, PA, 1992, pp. 303-15.
14. W. Kock and P. Paschen: *J. Met.*, 1989, vol. 41, p. 33.
15. R.J. Arsenault and A. Lawley: in *Work Hardening*, J.P. Hirth and J. Weertman, eds., Gordon and Breach Science Publishers, New York, NY, 1968, vol. 46, pp. 283-309.
16. J.B. Clark, J.R.K. Garrett, T.L. Jungling, and R.I. Asfahani: *Metall. Trans. A*, 1991, vol. 22A, pp. 2959-68.
17. J.B. Clark, J.R.K. Garrett, T.L. Jungling, and R.I. Asfahani: *Metall. Trans. A*, 1992, vol. 23A, pp. 2183-91.
18. S.I. Wright, G.T. Gray, and A.D. Rollett: *Metall. Mater. Trans. A*, 1994, vol. 25A, pp. 1025-31.
19. C.M. Lopatin, C.L. Wittman, J.P. Swensen, and P.F. Perron: in *High Strain Rate Behavior of Refractory Metals and Alloys*, R. Asfhani, E. Chen, and A. Crowson, eds., TMS-AIME, Warrendale, PA, 1992, pp. 241-47.
20. A.M. Rajendran, J.R.K. Garrett, J.B. Clark, and T.L. Jungling: *J. Mater. Shaping Technol.*, 1991, vol. 9, pp. 7-20.
21. A.M. Rajendran and J.R.K. Garrett: in *High Strain Rate Behavior of Refractory Metals and Alloys*, R. Asfahani, E. Chen, and A. Crowson, eds., TMS-AIME, Warrendale, PA, 1992, pp. 289-302.
22. D.H. Lassila and G.T. Gray: *3rd Int. Conf. on Mechanical and*

Physical Behavior of Materials under Dynamic Loading, J.D.P. IV, ed., 1991, vol. 1, pp. C3-19–C3-26.
23. C.L. Wittman, J.R.K. Garrett, J.B. Clark, and C.M. Lopatin: in *Shock-Wave and High-Strain-Rate Phenomena in Materials*, M.A. Meyers, L.E. Murr, and K.P. Staudhammer, eds., Marcel Dekker, Inc., New York, NY 1992, pp. 925-33.
24. G.T. Gray: *High-Pressure Science and Technology—1993 AIP Conf. Proc.*, S.C. Schmidt, J.W. Shaner, G.A. Samara, and M. Ross, eds., American Institute of Physics, New York, NY, 1994, vol. 309, pp. 1103-06.
25. J.N. Johnson, R.S. Hixson, D.L. Tonks, and G.T. Gray: *High-Pressure Science and Technology—1993 AIP Conf. Proc.*, S.C. Schmidt, J.W. Shaner, G.A. Samara, and M. Ross, eds., American Institute of Physics, New York, NY, 1994, vol. 309, pp. 1095-98.
26. D.L. Tonks, R.S. Hixson, J.N. Johnson, and G.T. Gray: *High-Pressure Science and Technology—1993 AIP Conf. Proc.*, S.C. Schmidt, J.W. Shaner, G.A. Samara, and M. Ross, eds., American Institute of Physics, New York, NY, 1994, vol. 309, pp. 997-1000.
27. M.D. Furnish, L.C. Chhabildas, and D.J. Steinberg: *High-Pressure Science and Technology—1993 AIP Conf. Proc.*, S.C. Schmidt, J.W. Shaner, G.A. Samara, and M. Ross, eds., American Institute of Physics, New York, NY, 1994, vol. 309, pp. 1099-1102.
28. P.S. Follansbee: in *Metals Handbook*, ASM, Metals Park, OH, 1985, vol. 8, pp. 198-203.
29. P.S. Follansbee and U.F. Kocks: *Acta Metall.*, 1988, vol. 36, pp. 81-93.
30. G.T. Gray: in *Modeling the Deformation of Crystalline Solids*, T.C. Lowe, A.D. Rollett, P.S. Follansbee, and G.S. Daehn, eds., TMS-AIME, Warrendale, PA, 1991, pp. 145-58.
31. K.S. Vecchio and G.T. Gray: *High-Pressure Science and Technology—1993 AIP Conf. Proc.*, S.C. Schmidt, J.W. Shaner, G.A. Samara, and M. Ross, eds., American Institute of Physics, New York, NY, 1994, vol. 309, pp. 1213-16.
32. G.T. Gray, P.S. Follansbee, and C.E. Frantz: *Mater. Sci. Eng.*, 1989, vol. A111, pp. 9-16.
33. D.I. Bolef: *J. Appl. Phys.*, 1961, vol. 32, p. 100.
34. R.W. Anderson and S.E. Bronisz: *Acta Metall.*, 1959, vol. 7, pp. 645-46.
35. C.S. Barrett and R. Bakish: *Trans. AIME*, 1958, vol. 212, pp. 122-23.
36. G.T. Gray: in *High Pressure Shock Compression of Solids*, J.R. Asay and M. Shahinpoor, eds., Springer-Verlag, New York, NY, 1993, pp. 187-215.
37. S.-R. Chen and G.T. Gray: Los Alamos National Laboratory, Los Alamos, NM, unpublished research, 1994.
38. U.F. Kocks: in *The Mechanics of Dislocations*, E.C. Aifantis and J.P. Hirth, eds., ASM, Metals Park, OH, 1985, pp. 81-83.
39. J.N. Johnson: *High-Pressure Science and Technology—1993 AIP Conf. Proc.*, S.C. Schmidt, J.W. Shaner, G.A. Samara, and M. Ross, eds., American Institute of Physics, New York, NY, 1994, vol. 309, pp. 1145-48.
40. Z.S. Basinski, M.S. Duesbery, and R. Taylor: *Phil. Mag.*, 1970, vol. 21, pp. 1201-21.
41. U.F. Kocks: in *Unified Constitutive Equations for Creep and Plasticity*, A.K. Miller, ed., Elsevier Press, New York, NY, vol. 1987, pp. 1-88.
42. J.R. Low and A.M. Turkalo: *Acta Metall.*, 1962, vol. 10, pp. 215-27.
43. W.G. Johnston and J.J. Gilman: *J. Appl. Phys.*, 1960, vol. 31, pp. 632-43.
44. J.R. Low and R.W. Guard: *Acta Metall.*, 1959, vol. 7, pp. 171-79.
45. D.K. Bowen, J.W. Christian, and G. Taylor: *Can. J. Phys.*, 1967, vol. 45, pp. 903-38.
46. W.A. Spitzig and T.E. Mitchell: *Acta Metall.*, 1966, vol. 14, pp. 1311-23.
47. U.F. Kocks: *Proc. Conf. on Dislocations and Properties of Real Materials*, The Institute of Metals, London, 1985, vol. 323, p. 125.